Adsorption of Radon on Metal Surfaces: A Model Study for Chemical Investigations of Elements 112 and 114

R. Eichler*,† and M. Schädel

Gesellschaft für Schwerionenforschung, Planckstrasse 1, 64291 Darmstadt, Germany

Received: October 4, 2001; In Final Form: March 4, 2002

The adsorption properties of Rn on polycrystalline surfaces of the transition metals Cu, Ag, Au, Ni, and Pd are investigated experimentally by vacuum thermochromatography. This experimental approach provides a fast separation of short-lived nuclides of volatile elements on clean metal surfaces. The adsorption enthalpies of Rn are quantified from the experimental results using a thermodynamic equilibrium model and a Monte Carlo based kinetic model of mobile adsorption, developed in this work. The experimentally observed strength of Rn adsorption is given by the sequence: Ni > Pd ≈ Cu > Au > Ag. The obtained adsorption data are compared with results from empirical calculations of the weak interaction of closed shell atoms with metallic surfaces. An empirical model, which was developed on the basis of experimental adsorption data of Ne, Ar, Kr, and Xe, is extended in order to calculate the adsorption enthalpies of Rn. An excellent agreement is found between model results and the experimental data for the adsorption of Rn on Ag, Au, Ni, and Pd. Extending the model furthermore to the hypothetically noble-gas such as super heavy elements 112 and 114, their adsorption enthalpies on Cu, Ag, Au, Ni, and Pd are predicted. The results and the experimental approach are discussed in view of the experimental investigation of gas-phase chemical properties of the transactinide elements 112 and 114.

1. Introduction

The adsorption of the light noble gases caught great scientific attention in the past. It was mainly driven by progress in experimental techniques and methods applied in the surface sciences. Investigations of sorption media for noble gases permitted further improvements in cryogenic pumping technology. Since noble-gas fission products (^{85}Kr and ^{133,135}Xe) are released from nuclear power plants and during nuclear fuel processing, the knowledge of their adsorption properties is an important aspect in radiation protection. Hence, the adsorption properties of neon, argon, krypton, and especially of xenon on a variety of surface materials are well-investigated (see, e.g., refs 1−9).

The radioactive noble gas radon (^{220,222}Rn) is known to be one of the largest radiation sources accountable for more than one-third of the natural radiation dose, received by the general public.[10] Gas adsorption techniques are applied for it's monitoring. The results of our work represent a significant contribution to the selection of metallic adsorbents for Rn.

Earliest works describing the condensation of Rn go back to the beginning of the past century.[11,12] Further works[13−16] were devoted to the condensation of Rn on different surfaces. Later, the observed differences of the deposition temperatures on a variety of surface materials have been attributed to an adsorption process instead of condensation.[17] More recently, the adsorption behavior of Rn on different surfaces was studied by gas thermochromatography using various carrier gases.[18−20]

In this work we report on the investigation of adsorption properties of Rn on transition metal surfaces. This study has been conducted to prepare chemical investigations of the elements 112 (E112) and 114 (E114). Evidence for the existence of isotopes of E112 and E114 with half-lives long enough to study their chemical behavior was obtained in the investigation of heavy ion induced fusion reactions[21−25] of ^{48}Ca with ^{238}U, ^{242,244}Pu, and ^{248}Cm. Since the production rates of the observed isotopes of E112 and E114 are in the order of only several atoms per week, exceptionally sensitive and efficient experimental chemical techniques have to be developed. The goal of these chemical studies is the arrangement of the transactinide elements in the periodic table.

For the heaviest elements, calculations of electron properties predict increasingly strong relativistic effects.[26−29] Due to the high nuclear charge relativistic velocities are expected for the s- and $p_{1/2}$-electrons leading to a contraction and thus to an energetic stabilization of the electrons in these spherical orbitals. As a consequence, the nuclear charge is more shielded. Therefore, the nonspherical $p_{3/2}$- and the d-electron orbitals are destabilized and expand. These effects lead to the prediction of shell closures in the relativistic valence electron orbitals 7s of E112 and 7s $7p_{1/2}$ of E114, which may strongly influence their chemical behavior. Therefore, E112 and E114 are predicted to be chemically inert and volatile elements, similar to noble gases.[30] Other theoretical approaches[31] indicate a noble, but metallic character for these elements, more similar to their homologues in groups 12 and 14 of the periodic table, mercury and lead, respectively. The expected high volatility would allow investigations of E112 and E114 ideally with gas-phase chemical methods in their elemental state. Studying their gas-adsorption behavior on metal surfaces[31,32] it should be possible to prove, whether the chemical behavior of these elements is metallic or whether strong relativistic effects render E112 and E114 to behave similar to noble gases.

Recently, a first attempt to experimentally investigate the adsorption properties of E112 on Au and Pd surfaces was made[33]

† Presently at Paul Scherrer Institut, CH-5232 Villigen. E-mail: robert.eichler@psi.ch.

10.1021/jp015553q CCC: $22.00
Published on Web 04/27/2002

using the isotope $^{283}112$, which decays by spontaneous fission (SF).[21] This experiment was conducted assuming that E112 behaves chemically like a noble metal. Thus, a deposition of E112 on Au- or Pd-coated detector surfaces at room temperature was expected. No spontaneous fission decays have been observed on the metallic detector surfaces. However, the experiment did not give an unambiguous answer about physical or chemical properties of E112.

In preparation of further experimental chemical investigations of E112 and E114 our study has a 2-fold interest: First, element Rn represents the noble gas, which should behave most similar to the hypothetically noble gas elements E112 and E114. Hence, it is well suited as a model element. Second, due to their decay properties, ^{212}Bi and ^{212}Po disturb or even disable the unambiguous detection of the heaviest elements by measurement of correlated α-decay chains. ^{220}Rn, the precursor of these disturbing isotopes, is produced in multinucleon transfer reactions from actinide targets as a byproduct of the fusion reactions with ^{48}Ca beam at much higher production rates[34] compared to those of E112 or E114. Therefore, ^{220}Rn has to be separated fast and effectively from E112 and E114.

Coverage of a broad temperature range applied to the stationary metallic phases is required for the gas-phase adsorption studies of E112 and E114. The differentiation between either a metallic or a noble-gas character of these superheavy elements can only be achieved using clean metallic surfaces in the adsorption chromatography process. Our experimental results show that these requirements can easily be fulfilled by the vacuum thermochromatography technique performed in a temperature region from 298 K down to 60 K.

A set of metals is selected in this work as chromatographic surfaces, representing a very noble metal (Au) but also metals for which a surface oxidation can be expected (Ag, Pd, Ni, and Cu). Thus the influence of surface oxidation processes on the adsorption properties of noble gas elements on these metallic surfaces are investigated using the model element Rn.

2. Experimental Section

The method of vacuum thermochromatography was already successfully applied for the separation of volatile elements and compounds at the on-line mass separator OSIRIS[35−37] and for adsorption studies of various elements on metallic surfaces.[38−40] Figure 1 shows a schematic view of the vacuum thermochromatography setup used in this work. The vacuum chamber (1) was evacuated by a turbo molecular pump setup (2) and a modified double stage cryogenic pump (3) to a pressure of about 3×10^{-5} Pa, well below the critical pressure, needed for molecular flow conditions. The pressure was monitored using an ionization gauge (4). A copper tube (5) was mounted on top of the cold head of the cryogenic pump. The thermochromatography experiments were carried out in quartz tubes (6), which were covered inside by thin metal foils (7). The quartz tube was then placed into the copper tube. A temperature gradient from T_1=273 K to T_4=20 K was obtained outside along the copper tube. The upper temperature (T_1) was forced by an oven (8). The stability of this temperature gradient was monitored by a stationary thermocouple (T_2). The temperature gradient from 230 to 60 K, obtained inside of the chromatography columns, was monitored by a moveable Teflon insulated thermocouple (T_3).

Either $^{nat.228/232}ThO_2$ (2 g as powder), emanating ^{220}Rn ($T_{1/2}$ = 55.6 s), or $^{227}Ac_2O_3$ (about 2×10^{-3} μg, deposited on a Pt-foil), emanating ^{219}Rn ($T_{1/2}$ = 3.96 s), were used as Rn sources (11). After about 15 h temperature equilibrium conditions were established along the chromatographic column. By opening the valve (12) to the emanation source the experiment was started. The emanating Rn isotopes entered the chromatographic column. During the experiments ^{220}Rn and ^{219}Rn decayed to the much less volatile nuclides ^{216}Po ($T_{1/2}$ = 0.15 s) or ^{215}Po ($T_{1/2}$ = 1.78 ms), respectively. These decay products were instantly deposited or kept adsorbed on the chromatographic surface. Subsequently they decayed by α-decay to ^{212}Pb ($T_{1/2}$ = 10.64 h) or ^{211}Pb ($T_{1/2}$ = 36.1 min), respectively. Hence, the deposition pattern of the Rn isotopes along the temperature gradient was "frozen". To obtain sufficiently high count rates along the chromatography columns, the experiment duration (t_{exp}) was adjusted to the half-life of the long-lived ^{212}Pb or ^{211}Pb, respectively. Afterward the chromatography column was removed from the vacuum chamber and the γ-emission of the nuclides ^{212}Pb (E_γ = 238 keV) and ^{211}Bi ($T_{1/2}$ = 2.17 min, E_γ = 351 keV, the equilibrium daughter activity of ^{211}Pb), were measured using an HPGe (high purity germanium) γ-detector. A longitudinal resolution of 1 cm was obtained along the chromatographic column by means of a lead collimator window in front of the detector.

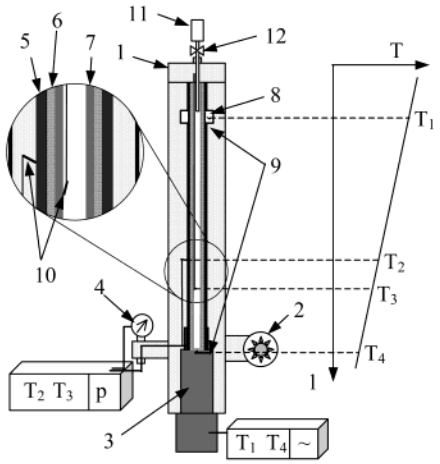

Figure 1. Schematic view of the vacuum thermochromatography setup and the temperature gradient (1) vacuum chamber, (2) turbo molecular pump, (3) cryogenic pump, (4) ionization gauge, (5) copper tube ($\varnothing_i$ = 5 mm) mounted onto the head of the cryogenic pump, (6) quartz tube ($\varnothing_i$ = 3.75 mm), (7) metal foil inlay, (8) oven, (9) thermocouples controlling the temperature gradient (T_1 the temperature of the head of cryogenic pump; T_4 the temperature of the oven), (10) monitoring thermocouples (T_2 stationary, outside on the copper tube; T_3 moveable, inside along the column), (11) emanation source of ^{220}Rn or ^{219}Rn ($^{232}ThO_2$, $^{227}Ac_2O_3$), (12) valve.

In a first experiment, the adsorption of Rn on the pure quartz surface was studied (Table 1, Series O). Next, the quartz columns were covered inside with thin (∼0.025 mm) metal foils yielding a cylindrical metallic chromatography surface with an inner diameter of 3.5 mm. Depending on the pretreatment of the chromatography columns, which had to be accomplished outside of the vacuum thermochromatography setup, the experiments are divided into four different experimental series:

A. Adsorption on untreated metal surfaces.

B. Adsorption on oxidized surfaces. The metal surfaces were heated for 5 min to 1000 K in air flowing at 100 mL/min.

C. Adsorption on reduced metallic surfaces with annealing. The columns were heated for about 2 h to 1000 K in a gas mixture of N_2+H_2 (90:10 vol %) flowing at100 mL/min and subsequently for about 10 min to 1000 K in a He flow of 100 mL/min.

D. Adsorption on reduced metallic surfaces without annealing. The metal columns were heated for about 2 h to 1000 K in a

TABLE 1: Experimental Parameters and Results Together with the Evaluated Adsorption Enthalpies for Each Experiment[a]

series	isotope	surface	surface treatment	T_{dep}, K	t_{exp}, h	$-\Delta H_{ads}$(ther), kJ/mol	$-\Delta H_{ads}$(kin), kJ/mol
O	^{219}Rn	SiO_2	no	96	3.5	19	22
A	^{219}Rn	Cu	no	131	3.5	26	30
	^{219}Rn	Ag	no	102	3	22	24
	^{220}Rn	Au	no	118	16	25	30
	^{220}Rn	Pd	no	90	15	20	23
	^{220}Rn	Ni	no	87	15	21	23
B	^{219}Rn	Cu	air	126	3	25	29
	^{219}Rn	Ag	air	98	3	19	21
	^{219}Rn	Au	air	164	3	32	36
	^{219}Rn	Pd	air	111	3	22	25
	^{219}Rn	Ni	air	122	3	24	28
C	^{219}Rn	Cu	H_2+N_2/He	183	3	37	40
	^{219}Rn	Ag	H_2+N_2/He	99	3	19	23
	^{219}Rn	Au	H_2+N_2/He	148	3	29	33
	^{219}Rn	Pd	H_2+N_2/He	178	3	36	40
	^{219}Rn	Ni	H_2+N_2/He	187	3	38	43
D	^{220}Rn	Cu	H_2+N_2	167	24	37	41
	^{219}Rn	Ag	H_2+N_2	107	3	21	24
	^{219}Rn	Au	H_2+N_2	148	3	29	33
	^{220}Rn	Pd	H_2+N_2	173	17	38	42
	^{220}Rn	Ni	H_2+N_2	177	50	40	43

[a] The adsorption enthalpies, ΔH_{ads} have been evaluated from the deposition temperatures, T_{dep}, using the thermodynamic equilibrium model of mobile adsorption ($-\Delta H_{ads}$(ther)) and the microscopic kinetic Monte Carlo model ($-\Delta H_{ads}$(kin), see text for description).

gas mixture of N_2+H_2 (90:10 vol %) flowing at 100 mL/min, but the treatment with He was omitted.

The main experimental data are listed in Table 1.

3. Evaluation of Adsorption Enthalpies

3.1. Thermodynamic Equilibrium Model of Mobile Adsorption. At molecular flow conditions the Rn atoms are moving in both directions along the column. The deposition of the atoms is mainly driven by the temperature-dependent adsorption−desorption equilibrium of Rn on the stationary surface and by the lifetime of the Rn atoms. The time the Rn atoms remain in the gaseous state is short. It mainly depends on the temperature and on the dimensions of the column. At the deposition temperature, T_{dep}, the residence time of the Rn atoms in the adsorbed state growth to be in the order of their radioactive lifetime. From T_{dep} observed in the experiment and from the selected experimental parameters, the adsorption enthalpy of Rn at zero surface coverage on the metal surfaces, ΔH_{ads}, was evaluated, using a thermodynamic equilibrium model of vacuum thermochromatography, based on principles of ideal linear gas chromatography.[40] This model assumes a corrected partition coefficient, which equals the standard equilibrium constant of the adsorption equilibrium corrected by the quotient of the sizes of both phases, the surface (s) and the gas phase (v). The corrected partition coefficient is the essential quantity describing the distribution of a gaseous species between both phases.

In the adsorbed state the main vibration of an atom is assumed to be perpendicular to the surface and in resonance with the solid-state surface phonon vibrations of the material.[41−44] We included this individuality of each metal surface, combining the thermodynamic equilibrium model of adsorption with the model of mobile adsorption at zero surface coverage.[44] In this model the change of the number of degrees of freedom occurring during the adsorption process of a gaseous atom or molecule is quantified by the mobile adsorption entropy, which can be calculated using eq 3. The values ν_b of the metals[45] used for this calculation are compiled in Table 2.

TABLE 2: The Enthalpies of Adsorption of Rn on Polycrystalline Metal Surfaces

	Rn						
metal	ν_b, $\times 10^{12}$ s^{-1}	IP eV	$-\Delta H_{ads}$ (ther), kJ/mol	$-\Delta H_{ads}$ (kin), kJ/mol	−EB, kJ/mol	$-\Delta H^M_{ads}$, kJ/mol	Xe $-\Delta H^M_{ads}$, kJ/mo
Cu	6.7	7.72	37 ± 2	40 ± 2	37	25 ± 2	21
Ag	4.65	7.57	20 ± 2	23 ± 2	36	26 ± 2	21.5
Au	4.2	9.22	29 ± 2	33 ± 2	41	33 ± 2	27.5
Pd	6.4	8.33	37 ± 2	41 ± 2	38	35 ± 2	29
Ni	8.1	7.63	39 ± 2	43 ± 2	36	37 ± 2	31

[a] The adsorption enthalpies of Rn on metal surfaces, which have been evaluated from the experimental data using the thermodynamic (ΔH_{ads}(ther)) and the kinetic model Monte Carlo model (ΔH_{ads}(kin)), are presented. The adsorption enthalpies, which were calculated applying a van der Waals model (EB)[65] and an extended empirical model of Miedema et al.[6] (ΔH^M_{ads}), are added. The basic values of this model, the adsorption enthalpies of Xe on the investigated metals ($-\Delta H^M_{ads}$(Xe)), are included. For each metal, the ionization potential (IP) and the maximum surface phonon frequency (ν_b), used in this work, are given.

Thus, the k_i used so far in the thermodynamic equilibrium model of vacuum thermochromatography:[40]

$$k_i = \frac{h}{k_B T}\sqrt{\frac{RT}{2\pi M}}\frac{s}{v}\exp\left(\frac{-\Delta H_{ads}}{RT}\right) \quad (1)$$

changes to

$$k_i = \frac{V}{S}\exp\left(\frac{\Delta S_{a,mob}}{R}\right)\frac{s}{v}\exp\left(\frac{-\Delta H_{ads}}{RT}\right) \quad (2)$$

with

$$\Delta S_{a,mob} = R\left\{\ln\left(\frac{S}{V}\frac{100}{\nu_b}\sqrt{\frac{RT}{2\pi M}}\right)+\frac{1}{2}\right\} \quad (3)$$

Using the model of "conductance" of a cylindrical tube for gaseous species at molecular flow conditions,[40] the final function for the calculation of the retention time of the chromatographic process is derived:

$$t_r = -\frac{1}{a}\int_{T_s}^{T_{dep}}\left\{\frac{3\pi(T-T_s)}{d^2 a\sqrt{\frac{2\pi RT}{M}}}\left(1+\frac{4}{d}\exp\left(\frac{\Delta S_{a,mob}}{R}\right)\exp\left(\frac{\Delta H_{ads}}{RT}\right)\right)\right\}dT \quad (4)$$

Applying numerical methods, e.g., Simpson's rule, this integral function have been solved for each experimental value of T_{dep}, with different ΔH_{ads} numerically, until the retention time equaled the mean radioactive lifetime of the Rn atoms:

$$t_\lambda = \frac{T_{1/2}}{\ln(2)} \quad (5)$$

where a = temperature gradient (negative), K/m; d = inner diameter of the chromatographic column, m; k_i = corrected partition coefficient, dimensionless; k_B = Boltzmann constant, J K^{-1}; h = Planck constant, J s; ΔH_{ads} = adsorption enthalpy at zero surface coverage, J mol^{-1}; M = molecular weight, kg mol^{-1}; ν_b = maximum phonon frequency of the metal lattice,[45] s^{-1}; R = gas constant 8.31441 J mol^{-1} K^{-1}; s = inner surface of the column per cm column length, m^2; $\Delta S_{a,mob}$ = entropy of

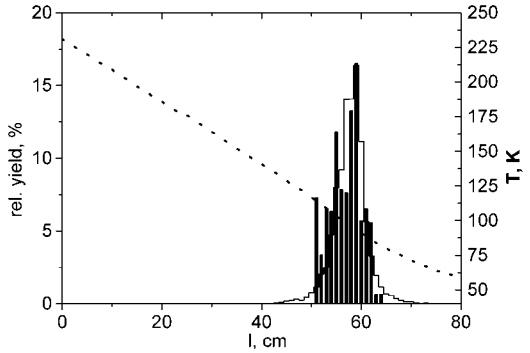

Figure 2. Vacuum thermochromatogram of ^{219}Rn on a polycrystalline Ag surface treated by heating the metal in a reducing gas mixture of H_2/N_2 at 1000 K. Presented are the experimentally obtained Rn distribution along the chromatographic column as black bars and the Monte Carlo simulated Rn distribution as a stepped line. The temperature gradient is shown as a dotted line.

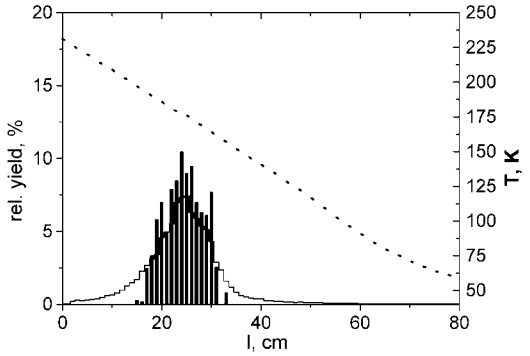

Figure 3. Vacuum thermochromatogram of ^{220}Rn on a polycrystalline Ni surface treated by heating the metal in a reducing gas mixture of H_2/N_2 at 1000 K. Presented are the experimentally obtained Rn distribution along the chromatographic column as black bars and the Monte Carlo simulated Rn distribution as a stepped line. The temperature gradient is shown as a dotted line.

mobile adsorption, J mol^{-1} K^{-1}; T = temperature, K; $T_{1/2}$ = half-life of the adsorbate, s; T_{dep} = deposition temperature, K; T_s = starting temperature of the gradient, K; t_r = chromatographic retention time, s; t_λ = mean radioactive lifetime, s; v = inner volume of the column per cm column length, m^3; V/S = standard state of the adsorption, m^{-1}.

For the calculation of ΔH_{ads}(ther) a linear temperature gradient have been approximated from the real experimental conditions (see Figures 2 and 3) to be -230 K/m.

3.2. Microscopic Kinetic Model of Mobile Adsorption. Similar to the Monte Carlo simulation of gas thermochromatography,[46] a Monte Carlo simulation of idealized microscopic adsorption and desorption processes of single atoms in an evacuated cylindrical tube was developed. The randomly selected values were the lifetime of the atom, τ_λ, the residence time of the atom in the adsorbed state, τ_a, and the solid angles of the desorption, θ and φ.

τ_λ has a logarithmic distribution based on the radioactive decay law:

$$P(\tau_\lambda) = \frac{\ln(2)}{T_{1/2}} \exp\left(\frac{-\tau_\lambda \ln(2)}{T_{1/2}}\right) \qquad (6)$$

τ_a has the same logarithmic distribution with a mean residence time, τ_{am}, of the atom in the adsorbed state, which is calculated using a Frenkel-type equation for a given temperature:

$$\tau_{am} = \frac{1}{\nu_b} \exp\left(\frac{-\Delta H_{ads}}{RT}\right) \qquad (7)$$

For consistency with the thermodynamic equilibrium model of mobile adsorption, the maximum phonon frequencies of the metal lattices,[45] ν_b, have been used to estimate the preexponential factor of the desorption kinetics.

The solid angles, θ and φ, of desorption of atoms from a plane surface into an evacuated volume describe the direction of the straight trajectory of the desorbed atom through the volume. The geometrical dimensions of the column limit the length of this trajectory. θ and φ are assumed to be distributed according to the cosine law:[47]

$$P(\varphi) = \cos(\varphi) \qquad \text{and} \qquad P(\theta) = \cos(\theta) \qquad (8)$$

The velocity of the Rn atoms in the gas phase was derived as the arithmetic mean velocity $\bar{v}$ from a Maxwell−Boltzmann distribution, which, for a given M, only depends on the temperature:

$$\bar{v} = \sqrt{\frac{8RT}{\pi M}} \qquad (9)$$

Usually, a sticking coefficient is introduced into a kinetic adsorption model, describing the probability for the occurrence of a real adsorption process on the surface instead of a scattering process with no residence time of the adsorbate at the surface. A sticking coefficient of >0.9 for Xe on Pd at a surface temperature of 77 K and a gas temperature of 300 K over a broad range of surface coverage was measured.[48] Sticking coefficients of almost unity at a low surface coverage have been determined[49] for the Xe adsorption on W at surface temperatures of 60 and 65 K and gas temperatures between 110 and 300 K. Therefore, the sticking coefficient in our Monte Carlo simulation was assumed to be unity.

A large number of atoms (typically 10000) with a given ΔH_{ads} are calculated to undergo adsorption and desorption processes between the surface and the gas phase. The geometry of the chromatographic surface was assumed to be ideally cylindrical with an inner diameter 3.5 mm and 0.8 m length. The real measured temperature gradient along the chromatography column was used in these simulations. The simulated chromatography process is proceeded for each atom until τ_λ or the end of the experiment, t_{exp}, is reached. The whole simulation procedure was repeated with different ΔH_{ads} until the maximum of the simulated deposition peak overlapped with the maximum of the deposition yield measured experimentally (see Figures 2 and 3).

4. Results and Discussion

4.1. Experimental Results. The original result of each thermochromatography experiment is an internal thermochromatogram (see, e.g., black bars in Figures 2 and 3) representing the distribution of the adsorbate along the chromatographic column. The deposition temperatures, T_{dep}, of Rn on the different surfaces have been determined to be the temperatures at the position, where the maxima of the deposition peaks were measured. This determination has an experimental uncertainty of about ±2 cm (i.e., ±6 °C) for the upper part (0−40 cm) of the column, where the peaks are broad (see Figure 2) and about ±1 cm (i.e., ±3 °C) for the lower part (40−80 cm) of the column, where the peaks are sharper (see Figure 3). The T_{dep} determined in every experiment are presented in Table 1 together with the adsorption enthalpies, evaluated from these T_{dep} using

the thermodynamic and the kinetic model of mobile adsorption, ΔH_{ads}(ther) and ΔH_{ads}(kin), respectively.

The surfaces of grinded metal foils are polycrystalline. A stronger interaction of the submonolayer adsorbate with the surface was observed for the adsorption of Xe on a stepped Pt surface.[50−54] This was explained by adsorption on surface steps, where a higher coordination of the Xe atom to Pt atoms is expected.[50−53] In contrast, a preferential adsorption of the Xe atoms on the upper step edges of a stepped Pt surface has been observed.[54] However, the occurring lateral surface diffusion of the noble gas atoms with typically small activation energy leads to the occupation of favorable adsorption sites. An excess of such surface irregularities compared to the number of Rn atoms can be expected in our experiments. However, it should be noted that it was not possible to heat the metal surfaces to temperatures above 298 K inside the vacuum thermochromatography setup. Thus, despite the low pressure of about 3×10^{-5} Pa, the most attractive adsorption sites of the metals remain occupied by gas molecules such as oxygen, nitrogen, carbon dioxide, and water from ambient air. Therefore, the experimentally obtained ΔH_{ads} are assumed to represent average adsorption enthalpies of the Rn interaction with the polycrystalline metal surfaces. This is corroborated by the surprisingly good agreement of the experimentally obtained peak shape in the thermochromatogram with the result of the Monte Carlo simulation (see Figures 2 and 3, stepped line), where an average ΔH_{ads} for all atoms and an ideal cylindrical chromatographic surface is assumed.

To investigate the effect of surface impurities of the metallic substrate on the adsorption behavior of Rn, four experimental series with different pretreatment of the metal surface were conducted (see Table 1):

A. Untreated surfaces are expected to be covered mainly by metal oxide layers, except for Au. Surface impurities due to the grinding process can be expected for all metals. These assumptions are in agreement with the observed weak adsorption interactions of Rn on these surfaces, comparable to the Rn behavior in pure quartz columns (see Table 1, series O).

B. While heating the metals in flowing air the surface oxidation was completed and oxidizable impurities were removed. In the experiments with Cu, Ag, Pd, and Ni the adsorption interactions of Rn were comparable to the first experiment series (A). These metal surfaces are indeed covered by oxide layers. The formation of oxide layers on the Au surface is not expected. The stronger adsorption interaction of Rn with Au in comparison to series A can be related to the purification of the Au surface from oxidizable and/or volatile impurities during the oxidation.

C. Heating the metals in the N_2+H_2 gas mixture reduced oxide layers on the surfaces. The formation of very rough and stepped surfaces was expected. An additional heating of the metals in He to 1000 K was conducted in order to remove adsorbed H_2 and N_2, to destroy hydride phases (Ni and Pd), to remove dissolved H_2 (Pd), and to anneal the surfaces. A strong increase of the adsorption interaction strength was observed for Cu, Pd and Ni compared to the corresponding experiments of series A and B. No strong changes were recognized for Au and Ag.

D. In the last experimental series the metal foils were also heated in a N_2+H_2 gas mixture up to 1000 K, but the additional treatment with He was omitted. No differences in comparison to the experiment series C were observed in these experiments. Obviously, the additional heating in He, did not strongly change of the surface properties of the metals.

TABLE 3: Proportionality Factors *C*(Z,Xe)[a]

element	$\alpha \times 10^{-24}$ cm^3	C_1(Z,Xe)	IP, eV	C_2(Z,Xe)	ΔH_{subl}, kJ/mol	C_3(Z,Xe)
He	0.22	0.12	24.6	0.098	0.07	0.032
Ne	0.39	0.17	21.6	0.17	2.5	0.17
Ar	1.64	0.52	15.8	0.52	9.0	0.52
Kr	2.48	0.72	14.0	0.72	12.4	0.72
Xe	4.01	1	12.1	1	17.4	1
Rn	4.853	1.11	10.5	1.31	19.5	1.11
E112	3.5	0.91	12	1.04	22	1.25
	4.3	1.04				
E114	5.8	1.2	8.5	2.00	42	2.36

[a] *C*(Z,Xe) connects empirically the enthalpy of adsorption of a closed shell atom (element) with the enthalpy of adsorption of Xe on the same metallic substrate. *C*(Z,Xe) for Z = Ne, Ar, Kr, and Xe are taken from ref 6. The factors *C*(Z,Xe) for Z = He, Rn, E112, and E114 have been obtained from three different empirical correlations of *C*(Z,Xe) with known or predicted properties of the adsorbate atoms: the enthalpy of sublimation (ΔH_{subl}), the polarizability (α), and the ionization potential (IP) (see Figures 4−6).

Only for the experimental series C and D the adsorption on clean metallic surfaces can be assumed. Therefore, the results from these experimental series represent the adsorption enthalpies of Rn on the transition metal surfaces (see Table 2, ΔH_{ads}(kin) and ΔH_{ads}(ther)). Both adsorption models, applied in this analysis yield similar results for ΔH_{ads}. The adsorption enthalpies of Rn on the metals Cu, Ag, Au, and Ni were determined experimentally for the first time. The evaluated adsorption enthalpy of Rn on Pd agrees very well with the data obtained by gas thermochromatography (-37 ± 4 kJ/mol).[18] The absolute value of the adsorption enthalpy quantifies the adsorption interaction strength of the adsorbate with the surface. The following sequence of the adsorption strength was determined: Ni > Pd ≈ Cu > Au > Ag.

The very similar deposition temperatures for ^{219}Rn and ^{220}Rn, despite their different half-lives indicate the adsorption chromatographic separation process in a vacuum at low temperatures to be fast. This was also deduced from vacuum thermochromatographic experiments at high temperatures in.[40] The similar deposition temperatures measured on the same metal at different experimental durations (see, e.g. Table 1, sections C and D, the experiments on Ni with t_{exp} of 3 and 50 h) indicate the metallic surfaces to be stable at the given vacuum conditions, which is a crucial point for the scientific and experimental concept of the investigation of E112 and E114.

4.2. Comparison with Empirical Models of Physisorption. Exact calculations of the interaction of closed shell atoms with hypothetical metal surfaces are available in the literature (see, e.g., refs 55−63). However, until now it is not possible to calculate the adsorption enthalpy of a noble gas atom on a real metal surface. Therefore, empirical models were used to estimate theoretical adsorption enthalpies of Rn on transition metal surfaces. Young and Crowell[64] give a critical review of such empirical methods, used for the calculation of physisorption interaction energies.

Assuming a pure van der Waals interaction, the binding energy, EB, of a polarizable closed shell atom (A) to a free electron metal can be calculated:[65,66]

$$EB = -\frac{E_A E_B}{(E_A + E_B)} \frac{\alpha}{8 r_e^3} \qquad (10)$$

where $E_{A/B}$ = effective excitation energy ($E_{A/B} = 1.57 IP_{A/B}$ from ref 67), α = polarizability of the closed shell atom (see Table 3), $IP_{A/B}$ = ionization potentials of the metal and the adsorbate

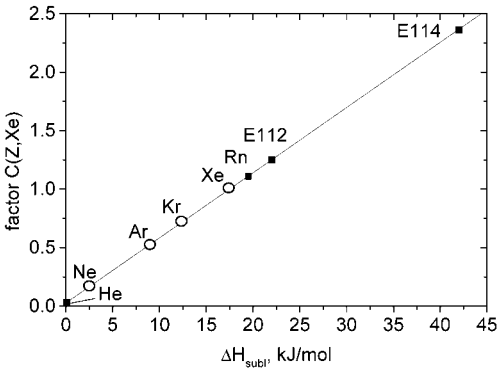

Figure 4. Empirical correlation of the factors C(Z,Xe) for the calculation of the adsorption enthalpies of noble gases on metals[6] with their enthalpies of sublimation (ΔH_{subl}) (grey circles) together with a least-squares fit (black line) and extrapolated data (black squares). For values, see Table 3.

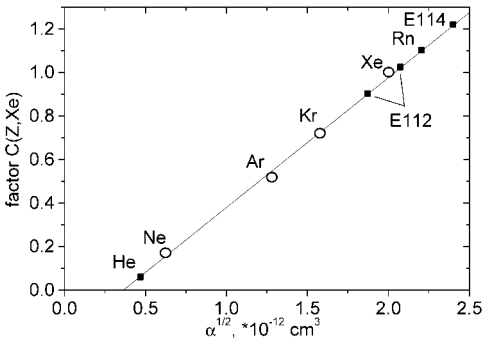

Figure 5. Empirical correlation of the factors C(Z,Xe) for the calculation of the adsorption enthalpies of noble gases on metals[6] with the square root of their polarizabilities (α) (grey circles) together with a least-squares fit (black line) and extrapolated data (black squares). For values, see Table 3.

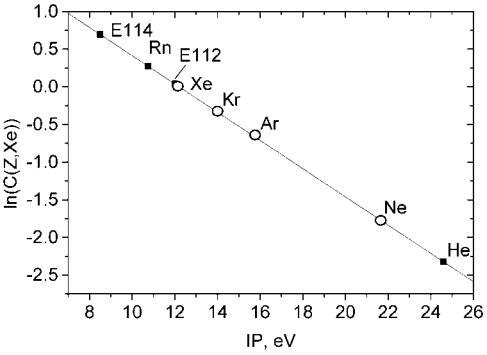

Figure 6. Empirical correlation of the natural logarithm of the factors C(Z,Xe) for the calculation of the adsorption enthalpies of noble gases on metals[6] with their ionization potentials (IP) (grey circles) together with a least-squares fit (black line) and extrapolated data (black squares). For values, see Table 3.

from[65] (see Table 3), and r_e = distance between the adsorbate and the substrate.

We used the van der Waals radii of Rn (224 pm)[69] and Xe (218 pm),[69] respectively, for the calculation of EB with eq 10. The resulting binding energies of Rn on the investigated metal surfaces are presented in Table 2. The calculated data agree well only for the adsorption of Rn on Pd and Cu with the experimental results. Among the other values of EB not even the trend determined experimentally in the adsorption interaction strength (Ni > Pd ≈ Cu > Au > Ag) is reproduced. Differing experimental results from results of such empirical binding energy calculations have been observed previously.[64] On the basis of observed changes of the surface work function of metals as a result of the adsorption of noble gases on their surface, an additional charge transfer no bond (CTNB) contribution to the physisorptive binding energy between the closed shell atom and the coordinating surface metal atoms have been suggested.[68] However, a theoretical approach to quantify this CTNB part is not available yet. Furthermore, the uncertainty of the adsorption distance r_e introduces a large error to this physisorption model.

Another empirical model was presented by Miedema et al.[6] They took the adsorption enthalpy of noble gases on metal surfaces as being proportional to the energy of adhesion. The calculated adsorption enthalpies of Xe on metal surfaces agree with literature data within an error range of about ±5%. The authors suggest, from the results of their calculations for the lighter noble gases, a linear dependence between the adsorption enthalpies of Ne, Ar, and Kr on metal surfaces and the empirically calculated adsorption enthalpies of Xe on the same metal surfaces:

$$\Delta H^{M}_{ads}(Z) = C(Z,Xe)\Delta H^{M}_{ads}(Xe) \qquad (11)$$

The adsorbate dependent factors C(Z,Xe) adopted from ref 6 for Z = Ne, Ar, and Kr are compiled in Table 3. To extend these calculations to other closed shell atoms, we searched for empirical functional dependencies of these factors on individual properties of the adsorbates. We found clear empirical linear dependencies between the factors C(Z,Xe) for Z = Ne, Ar, Kr, and Xe and the enthalpies of sublimation[70,71] (see Figure 4), the square root of the polarizabilities[72,73] (see Figure 5). The natural logarithm of C(Z,Xe) was found to correlate linearly with the ionization potentials[65] (see Figure 6). Subsequently, the factors C(Z,Xe) for the calculation of the adsorption enthalpies (ΔH^{M}_{ads}) of closed shell atoms Z (Z = He, Rn) on different metal surfaces have been obtained from these empirical linear correlations by extrapolation (see Figures 4-6; for values, see Table 3). The ΔH^{M}_{ads} of Rn on the metal surfaces of Cu, Ag, Au, Pd, and Ni were calculated using eq 11. The results are presented in Table 2 (Rn, $-\Delta H^{M}_{ads}$). The values of the calculated adsorption enthalpies of Xe on the metals from,[6] which have been used in eq 11, are also included in Table 2 (Xe, $-\Delta H^{M}_{ads}$). Obviously, the results from this extended empirical model are in very good agreement with our experimental results, ΔH_{ads}(therm) and ΔH_{ads}(kin). One exception is the adsorption enthalpy of Rn on Cu. This discrepancy between the model results and the experimental data can be explained by the surface roughness of the Cu foil used in our experiments. Due to a deep layer surface oxidation of Cu and its subsequent reduction with H_2, the surface becomes macroscopically very rough. This much larger interaction surface is not considered in the models for the evaluation of the adsorption enthalpy from our experimental results. Applying the thermodynamic equilibrium model (see section 3.1) and assuming the calculated ΔH^{M}_{ads} to be the real adsorption enthalpy of Rn on Cu, it is possible to estimate a surface enlargement of Cu during the pretreatment by a factor of about 1000.

The good agreement with our other experimental results encouraged us to use this model for a prediction of the adsorption enthalpies of E112 and E114 on different metal surfaces, assuming hypothetically a noble-gas-like behavior of these elements. For the empirical deduction of C(E112,Xe) and C(E114,Xe), predicted properties of the elements E112 and E114 have been used: the polarizabilities,[66,74] the sublimation enthalpies,[31,75,76] and the ionization potentials[77,78] (for values, see Table 3). The extrapolations of C(E112,Xe) and C(E114,Xe)

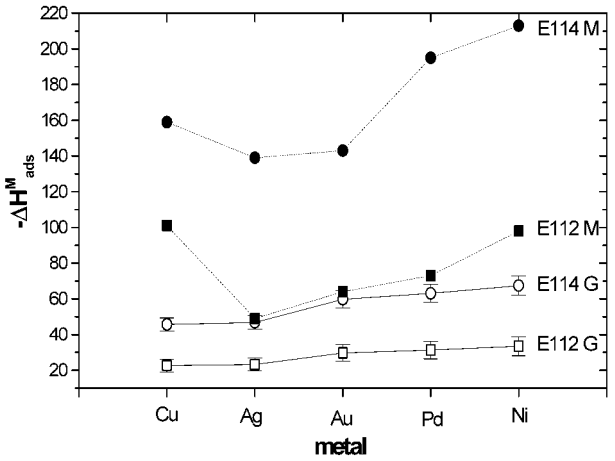

Figure 7. Predicted adsorption enthalpies (ΔH^{M}_{ads}) of E112 and E114 on metals. The values E112G and E114G (open symbols) have been calculated on the basis of the empirical model developed by Miedema et al.[6] The model was extended empirically to describe the physisorption of the hypothetically noble gases E112 and E114 on metals (for details see text). The values E112M and E114M (closed symbols) quantify the adsorption interaction of the hypothetically noble metals E112 and E114 with the investigated transition metal surfaces. The values have been taken from Eichler.[80,81]

are shown in Figures 4−6. The predicted values for the adsorption enthalpies of E112 and E114 on Cu, Ag, Au, Ni, and Pd are presented in Figure 7. These values have to be distinguished from the adsorption enthalpies calculated with the Miedema model for metal−metal interactions,[79] which was applied to transactinide elements assuming a metallic behavior of E112 and E114.[80,81] The predicted values taken from[80,81] have been inserted into Figure 7 for comparison. The metallic interaction of the elements E112 and E114 with transition metal surfaces are expected to be much stronger and much more dependent on the nature of the metal surface.

5. Conclusion

The low temperature vacuum thermochromatography technique can be used for the investigation of adsorption interactions of very volatile atoms and molecules on a wide variety of surfaces. It provides crucial advantages for experiments with short-lived isotopes: fast separation, no carrier gases, clean metallic surfaces, and a very stable temperature gradient due to the good heat isolation in a vacuum. Additionally, the vacuum conditions are ideally suited for a high-resolution α- and SF-spectroscopy.

For the design of vacuum thermochromatographic experiments with transactinide elements and their compounds, the developed Monte Carlo simulation procedure can be applied to model the distribution of volatile atoms or molecules along chromatographic columns. This model can be easily adapted to different macroscopic geometric shapes of the stationary chromatographic phase.

For the first time, the adsorption enthalpies of Rn on polycrystalline Ag, Au, and Ni surfaces were experimentally determined. The known adsorption enthalpy of Rn on Pd[18] was confirmed. As expected the adsorption interaction of the investigated metals with Rn is strongly influenced by the surface oxidation of the metals.

The extended empirical model of Miedema et al.[6] describes the experimental results for the adsorption interaction strength of Rn with clean metal surfaces well. Thus, it can be used to estimate the adsorption interaction of noble-gas-like elements with metal surfaces.

The predicted adsorption enthalpies of the hypothetical noble gas elements E112 and E114 allow selecting the best-suited stationary phase for their on-line gas-phase chemical study. Using the vacuum thermochromatography technique, an unambiguous differentiation of either noble-gas-likeness as or metallic behavior of E112 and E114 can be achieved on all metal surfaces, studied in this work. The most efficient experimental approach in the chemical investigation of E112 and E114 is the application of the α- and SF-detectors directly as the stationary chromatographic phase.[33] For this purpose, the detector surface needs to be covered with the desired metal. However, this approach has some limitations in terms of the upper temperature at which the detectors are functioning (approximately 320 K). The expected deposition temperature region of 100−300 K for E112 on a Pd or Au surface is below this limit. Additionally, the possibility to remove the Pd oxide layers with a H_2 containing gas mixture already at room temperature makes Pd an ideal suited surface material for the demanding chemical experiments with E112, lasting several weeks. The deposition temperature regions for a physisorptive interacting E114 on Pd (350−420 K) or Au (300−375 K) are predicted to be too high for the use of common metal covered α- and SF-detectors as stationary surfaces. In this case coverage of the detectors with Ag moves the deposition region of E114 to much lower temperatures of about (220−290 K).

The predictions given in this work indicate that E114 can chemically clearly be separated from Rn. If E112 behaves as a noble metal, it can also be separated from Rn. The dilemma of the predicted similarity of a fictitious noble gas such as E112 to Rn and the experimental requirement to separate Rn from E112 cannot be solved applying chemical separation techniques. Physical separation methods as a gas-filled recoil separator or a velocity filter should assist to effectively preseparate E112 from Rn. However, the vacuum thermochromatography technique provides an excellent choice when coupled to such physical separators which work at low gas pressure or even at vacuum conditions. On the other hand, further investigations of spontaneous-fissioning isotopes of the element E112, e.g., $^{283}112$, for which the decay modes of the Rn daughter isotopes do not interfere, are envisaged. Even though, the unambiguous identification of an isotope at a one-atom-at-a-time scale only by detection of its spontaneous fission decay is complicated.

References and Notes

(1) Nieuwenhuys, B. E.; Sachtler, W. M. *Surf. Sci.* **1974**, *45*, 513.
(2) McElhiney, G.; Pritchard, J. *Surf. Sci.* **1976**, *60*, 397.
(3) Nieuwenhuys, B. E.; Sachtler, W. M. *J. Colloid Interface Sci.* **1977**, *58*, 65.
(4) Küppers, J.; Nitschke, F.; Wandelt, K.; Ertl, G. *Surf. Sci.* **1979**, *87*, 295.
(5) Glachant, A.; Bardi, U. *Surf. Sci.* **1979**, *87*, 187.
(6) Miedema, A. R.; Nieuwenhuys, B. E. *Surf. Sci.* **1981**, *104*, 491.
(7) Christmann, K.; Demuth, J. E. *Surf. Sci.* **1982**, *120*, 291.
(8) Wandelt, K.; Hulse, J. E. *J. Chem. Phys.* **1984**, *80*, 1340.
(9) Ishi, S.; Viswanathan, B. *Thin Solid Films* **1991**, *201*, 373.
(10) Biancotto, R.; Marinaro, M.; Tommasino, L. *Radiat. Prot. Dosim.* **1998**, *78*, 1−85.
(11) Curie, M.; Danne, J. *C. R. Acad. Sci.* **1903**, *136*, 364, 1314.
(12) Rutherford, E.; Soddy, F. *Philos. Mag.***1903**, *5*, 561.
(13) Bunzel, H. *Ber. Wien. Akad. IIa* **1906**, *115*, 21.
(14) Meyer, S.; Schweidler, E. *Ber. Wien. Akad. IIa* **1906**, *115*, 329.
(15) Laborde, A. *Radium* **1909**, *6*, 289.
(16) Boyle, R. W. *Philos. Mag.* **1910**, *20*, 955.
(17) Curie, M. *Die Radioaktivität*; Akademische Verlagsgesellschaft: Leipzig, 1912; pp 253−265.
(18) Eichler, B.; Son Chun, K. *Isotopenpraxis* **1985**, *21*, 180.
(19) Eichler, B.; Zimmermann, H. P.; Gäggeler, H. W. *J. Phys. Chem. A* **2000**, *104*, 3126.

(20) Eichler, R.; Eichler B. *PSI Scientific Report 2000: Particles and Matter*; Paul Scherrer Institute: Villigen, 2001; p 127. (PSI−Scientific Reports 2000: a CD-ROM version can be ordered at http://www.psi.ch/news_events/news_events_info_material.shtml.)

(21) Oganessian, Yu. Ts.; Yeremin, A. V.; Gulbekian, G. G.; Bogomolov, S. L.; Chepigin, V. I.; Gikal, B. N.; Gorshkov, V. A.; Itkis, M. G.; Kabachenko, A. P.; Kutner, V. B.; Lavrentev, A. Yu.; Malyshev, O. N.; Popeko, A. G.; Roac, J.; Sagaidak, R. N.; Hofmann, S.; Münzenberg, G.; Veselsky, M.; Saro, S.; Iwasa, N.; Morita, K. *Eur. Phys. J. A* **1999**, *5*, 63.

(22) Oganessian, Yu. Ts.; Utyonkov, V. K.; Lobanov, Yu. V.; Abdullin, F. Sh.; Polyakov, A. N.; Shirokovsky, I. V.; Tsyganov, Yu. S.; Gulbekian, G. G.; Bogomolov, S. L.; Gikal, B. N.; Mezentsev, A. N.; Iliev, S.; Subbotin, V. G.; Shukov, A. M.; Ivanov, O. V.; Buklanov, G. V.; Subotic, K.; Itkis, M. G. *Phys. Rev. C* **2000**, *62*, 041604(R).

(23) Oganessian, Yu. Ts.; Utyonkov, V. K.; Lobanov, Yu. V.; Abdullin, F. Sh.; Polyakov, A. N.; Shirokovsky, I. V.; Tsyganov, Yu. S.; Gulbekian, G. G.; Bogomolov, S. L.; Gikal, B. N.; Mezentsev, A. N.; Iliev, S.; Subbotin, V. G.; Shukov, A. M.; Buklanov, G. V.; Subotic, K.; Itkis, M. G.; Moody, K. J.; Wild, J. F.; Stoyer, N. J.; Stoyer, M. A.; Lougheed, R. W. *Phys. Rev. Lett.* **1999**, *83*, 3154.

(24) Oganessian, Yu. Ts.; Utyonkov, V. K.; Lobanov, Yu. V.; Abdullin, F. Sh.; Polyakov, A. N.; Shirokovsky, I. V.; Tsyganov, Yu. S.; Gulbekian, G. G.; Bogomolov, S. L.; Gikal, B. N.; Mezentsev, A. N.; Iliev, S.; Subbotin, V. G.; Shukov, A. M.; Buklanov, G. V.; Subotic, K.; Itkis, M. G.; Moody, K. J.; Wild, J. F.; Stoyer, N. J.; Stoyer, M. A.; Lougheed, R. W.; Laue, C. A.; Karelin, Ye. A.; Tatarinov, A. N. *Phys. Rev. C* **2000**, *63*, 011301(R).

(25) Oganessian, Yu. Ts.; Yeremin, A. V.; Popeko, A. G.; Bogomolov, S. L.; Buklanov, G. V.; Chelnokov, M. L.; Chepigin, V. I.; Gikal, B. N.; Gorshkov, V. A.; Gulbekian, G. G.; Itkis, M. G.; Kabachenko, A. P.; Lavrentev, A. Yu.; Malyshev, O. N.; Roac, J.; Sagaidak, R. N.; Hofmann, S.; Saro, S.; Giardina, G.; Morita, K. *Nature* **1999**, *400*, 242.

(26) Fricke, B.; Waber, J. T. *Act. Rev.* **1971**, *1*, 433.

(27) Pyykkö, P. *Chem. Rev.* **1988**, *88*, 563.

(28) Schwerdtfeger, P.; Seth, M. In *Encyclopaedia of Computational Chemistry*; Wiley: New York, 1998; Vol. 4, pp 2480−2499.

(29) Pershina, V. G. *Chem. Rev.* **1996**, *96*, 1977.

(30) Pitzer, K. *J. Chem. Phys.* **1975**, *63*, 1032.

(31) Eichler, B. *Kernenergie* **1976**, *19*, 307.

(32) Eichler, B.; Reetz, T. *Kernenergie* **1981**, *25*, 218.

(33) Yakushev, A. B.; Buklanov, G. V.; Chelnokov, M. L.; Chepigin, V. I.; Dmitiev, S. N.; Gorshkov, V. A.; Lebedev, V. Y.; Malyshev, O. N.; Ogannessian, Y. T.; Popeko, A. G.; Sokol, E. A.; Timokhin, A. N.; Vasko, V. M.; Yeremin, A. V.; Zvara, I.; Hübener, S.; Türler, A. *PSI Scientific Report 2000*; Villigen, 2001; 126. (PSI−Scientific Reports 2000: a CD-ROM version can be ordered at http://www.psi.ch/news_events/news_events_info_material.shtml.)

(34) Gäggeler, H.; Brüchle, W.; Brügger, M.; Schädel, M.; Sümmerer, K.; Wirth, G.; Kratz, J. V.; Lerch, M.; Blaich, T.; Herrmann, G.; Hildebrand, N.; Trautmann, N.; Lee, D.; Moody, K. J.; Gregorich, K. E.; Welch, R. B.; Seaborg, G. T.; Hoffman, D. C.; Daniels, W. R.; Fowler, M. M.; von Gunten, H. R. *Phys. Rev. C* **1986**, *33*, 33.

(35) Westgaard, L.; Rudstam, G.; Jonsson, O. C. *J. Inorg. Nucl. Chem.* **1969**, *31*, 3747.

(36) Grapengriesser, B.; Rudstam, G. *Radiochim. Acta* **1973**, *20*, 85.

(37) Rudstam, G.; Grapengriesser, B. *Radiochim. Acta* **1973**, *20*, 97.

(38) Eichler, B.; Buklanov, G. V.; Timokhin, S. N. *Kernenergie* **1987**, *30*, 11.

(39) Hildebrand, N.; Frink, C.; Greulich, N.; Hickmann, U.; Kratz, J. V.; Trautmann, N.; Herrmann, G.; Brügger, M.; Gäggeler, H.; Sümmerer, K.; Wirth, G. *Nucl. Instrum. Methods A* **1987**, *260*, 407.

(40) Gäggeler, H.; Eichler, B.; Greulich, N.; Herrmann, G.; Trautmann, N. *Radiochim. Acta* **1986**, *40*, 137.

(41) Gortel, Z. W.; Kreuzer, H. J.; Teshima, R. *Phys. Rev. B* **1980**, *22*, 512.

(42) Gortel, Z. W.; Kreuzer, H. J.; Teshima, R.; Turski, L. A. *Phys. Rev. B* **1981**, *24* (8), 4456.

(43) Armand, G.; Masri, P.; Dobrzysnski, L. *J. Vac. Sci.* **1971**, *9*, 705.

(44) Eichler, B.; Zvara, I. *Radiochim. Acta* **1982**, *30*, 233.

(45) Dederichs, P. H.; Schober, H.; Sellmeyer, D. J. *Landoldt Börnstein: Metalle, Board 13*; Springer-Verlag: Berlin, 1981.

(46) Zvara, I. *Radiochim. Acta* **1985**, *38*, 95.

(47) Knudsen, M. *Ann. Phys. 4* **1909**, *28*, 75.

(48) Palmberg, P. W. *Surf. Sci.* **1971**, *25*, 598.

(49) Wang, C.; Gomer, R. *Surf. Sci.* **1979**, *84*, 329.

(50) Pouthier, V.; Ramseyer, C.; Girardet, C. *Surf. Sci.* **1998**, *400*, 176.

(51) Widdra, W.; Trischberger, P.; Friess, W.; Menzel, D.; Payne, S. H.; Kreuzer, H. J. *Phys. Rev. B* **1998**, *57*, 4111.

(52) Rettner, C. T.; Bethune, D. S.; Schweizer, E. K. *J. Chem. Phys.* **1990**, *92*, 1442.

(53) Siddiqui, H. R.; Chen, P. J.; Guo, X.; Yates, J. T., Jr. *J. Chem. Phys.* **1990**, *92*, 7690.

(54) Horch, S.; Zeppenfeld, P. *Appl. Phys. A* **1995**, *60*, 147.

(55) Clarke, S.; Bihlmayer, G.; Blügel, S. *Phys. Rev. B* **2001**, *63*, 85416.

(56) Trioni, M. I.; Marcotulio, S.; Santoro, G.; Bortolani, V.; Palumbo, G.; Brivio, G. P. *Phys. Rev. B* **1998**, *58* (16), 11043.

(57) Boninsegni, N.; Cole, M. W.; Toigo, F. *Phys. Rev. Lett.* **1999**, *83*, 2002.

(58) Ossicini, S. *Phys. Rev. B* **1985**, *33*, 873.

(59) Lang, N. D. *Phys. Rev. Lett.* **1981**, *46*, 842.

(60) Müller, J. E. *Phys. Rev. Lett.* **1990**, *65*, 3021.

(61) Kleiman, G. G.; Landmann, U. *Phys. Rev. Lett.* **1973**, *31*, 707.

(62) Zaremba, E.; Kohn, W. *Phys. Rev. B* **1976**, *13*, 2270.

(63) Zaremba, E.; Kohn, W. *Phys. Rev. B* **1977**, *15*, 1769.

(64) Young, D. M.; Crowell, A. D. *Physical Adsorption of Gases*; Butterworth: London, 1962; pp 6−63.

(65) *CRC Handbook of Chemistry and Physics*, 79th ed.; CRC Press: Boca Raton, 1998.

(66) Eichler, B.; Eichler, R.; Gäggeler, H. W. *PSI Scientific Report 2000: Particles and Matter*; Paul Scherrer Institute: Villigen, 2001; p 128. (PSI−Scientific Reports 2000: a CD-ROM version can be ordered at http://www.psi.ch/news_events/news_events_info_material.shtml.)

(67) Pauling, L. *Science* **1961**, *134*, 15.

(68) Mignolet, J. C. P. *J. Chem. Phys.* **1953**, *32*, 1298.

(69) Pyykkö, P. *Chem. Rev.* **1997**, *97*, 597.

(70) Grosse, A. V. *J. Inorg. Nucl. Chem.* **1965**, *27*, 509.

(71) Cockett, A. H.; Smith, K. C. In *Comprehensive Inorganic Chemistry*; Bailar, J. C., Emeleus, H. J., Nyholm, R., Trotman-Dickenson, A. F., Eds.; Pergamon Press: Oxford, 1973; p 139.

(72) Nicklass, A.; Dolg, M.; Stoll, H.; Preuss, H. *J. Chem. Phys.* **1995**, *102*, 8942.

(73) Haettig, C.; Hess, B. A. *J. Phys. Chem. A* **1996**, *100*, 6243.

(74) Seth, M.; Schwerdtfeger, P.; Dolg, M. *J. Chem. Phys.* **1997**, *106*, 3623.

(75) Fricke, B. In *Structure and Bonding*; Springer-Verlag: Berlin, 1975; Vol. 21.

(76) Keller, O. L., Jr.; Burnett, J. L.; Carlson, T. A.; Nestor, C. W., Jr. *J. Phys. Chem.* **1970**, *74*, 1127.

(77) Eliav, E.; Kaldor, U.; Ishikawa, Y. *Phys. Rev. A* **1995**, *52* (4), 2765.

(78) Landau, A.; Eliav, E.; Ishikawa, Y.; Kaldor, U. *J. Chem. Phys.* **2001**, *114* (7), 2977.

(79) Miedema, A. R.; Dorleijn J. W. F. *Surf. Sci.* **1980**, *95*, 447.

(80) Eichler, B. *PSI Report 00-09*; Paul Scherrer Institute: Villigen, 2000. (PSI−Scientific Reports 2000: a CD-ROM version can be ordered at http://www.psi.ch/news_events/news_events_info_material.shtml.)

(81) Eichler, B. *PSI Scientific Report 2000: Particles and Matter*; Paul Scherrer Institute: Villigen, 2001; p 125. (PSI−Scientific Reports 2000: a CD-ROM version can be ordered at http://www.psi.ch/news_events/news_events_info_material.shtml.)